Predicting Survival in Extracorporeal Membrane Oxygenation Patients With Optical Microcirculation Sensing

Hsiao-Huang Chang, Yung-Chang Chen, Ting-Wei Chiang, Yi-Min Wang, and Chia-Wei Sun

***Abstract*—In this study, we propose a novel method to use functional near-infrared spectroscopy (NIRS) to monitor patients' lower limb microcirculation with extracorporeal membrane oxygenation (ECMO). We controlled the ECMO system's speed and measured hemodynamics using NIRS devices which attached to both calves at approximately 60% of the tibia length. Features from the collected blood oxygen data were extracted and utilized as machine learning inputs for classification. The patients were divided into two groups based on discharge and mortality. In venovenous (VV) ECMO, we found that the construction of the classification model based on the characteristics of this type with better discriminating ability can effectively distinguish the two groups.**

***Index Terms*—Near-infrared spectroscopy, extracorporeal membrane oxygenation, support vector machine, microcirculation.**

I. Introduction

THE human body's circulatory system is responsible for performing many physiological functions, including transporting oxygen and nutrients, removing metabolites, and maintaining temperature stability. It comprises the heart, lungs, arteries, veins, and microcirculation. Microcirculation is the terminal part of the circulatory system, and it is also the place where the material is exchanged between blood and tissue cells. Clinically, patients with acute and severe diseases are often unable to provide sufficient oxygen to maintain the metabolic needs of tissues in the body due to impaired cardiovascular function and thus causing shock. During shock, the peripheral vascular system will contract to ensure blood supply to the heart and brain, causing various pathological changes and even perfusion failure between body organs and tissue cells due to ischemia and hypoxia. Therefore, monitoring peripheral microcirculation changes in acute and critical patients helps clinicians evaluate and judge patients' physiological conditions [1], [2], [3], [4].

Extracorporeal membrane oxygenation (ECMO) is a lifesaving rescue treatment in refractory respiratory and cardiac failure [5], [6], [7], [8], [9], [10]. It can be divided into the following two basic types: venovenous (VV) and venoarterial (VA)-ECMO [11]. VV-ECMO removes blood from the inferior vena cava, passes it through the ECMO device, and returns it to the body via the femoral or jugular vein. It can replace the respiratory function of the lungs. Suppose the patient's heart function is normal, but there is a problem with lung function. In that case, this device is suitable for preventing the complications caused by arterial intubation [12], [13]; VA-ECMO removes blood from the inferior vena cava, passes it through the ECMO device, and returns it to the body via the femoral artery. It can provide heart pumping and respiratory function support. When patients experience sepsis or hypotension because of other factors, they will undergo treatment with this type of device. According to the data from the annual international Extracorporeal Life Support Organization (ELSO) Registry Reports through July 2020, a total of 57958 adult patients have received the ECMO device since 1990, of which approximately 60% of the patients were removed from the aid of the ECMO device, and 48.8% of patients survived and were discharged successfully [14]. Although ECMO has been effective in improving the survival rate of patients [15], there are still considerable risks and complications that are difficult to resolve after its use [16], [17], [18]. Currently, there is no reliable and immediate mechanism for detecting hemodynamic changes in the peripheral tissues. We can merely use basic physiological parameters to adjust the ECMO setting. Therefore, monitoring peripheral micro-circulation changes in acute and critical patients helps clinicians evaluate and judge patients' physiological status.

Manuscript received 29 September 2022; revised 6 November 2022; accepted 7 November 2022. Date of publication 25 November 2022; date of current version 7 December 2022. This work was supported by the National Science and Technology Council under Grants 109-2221-E-009-018-MY3, 111-2221-E-A49-047-MY3, 111-2622-E-A49-030, and 109-2811-E-009 -532 -MY3. *(Corresponding author: Chia-Wei Sun.)*

This work involved human subjects or animals in its research. Approval of all ethical and experimental procedures and protocols was granted by National Chiao Tung University (Currently, National Yang Ming Chiao Tung University) and Taipei Veterans General Hospital. (TVGHIRB-2019-02-007AC).

Hsiao-Huang Chang is with the Department of Surgery, Division of Cardiovascular Surgery, Taipei Veterans General Hospital, Taipei 11217, Taiwan (e-mail: shchang@vghtpe.gov.tw).

Yung-Chang Chen, Ting-Wei Chiang, and Yi-Min Wang are with the Biomedical Optical Imaging Lab, Department of Photonics, College of Electrical and Computer Engineering, National Yang Ming Chiao Tung University, Hsinchu 30010, Taiwan (e-mail: stanley4129889@gmail.com; ms954b23@gmail.com; hn0937@nycu.edu.tw).

Chia-Wei Sun is with the Department of Photonics and Institute of Biomedical Engineering, College of Electrical and Computer Engineering, National Yang Ming Chiao Tung University, Hsinchu 30010, Taiwan, and also with the Medical Device Innovation and Translation Center, National Yang Ming Chiao Tung University, Taipei 112304, Taiwan (e-mail: chiaweisun@nycu.edu.tw).

This article has supplementary material provided by the authors and color versions of one or more figures available at https://doi.org/10.1109/JSTQE.2022.3223057.

Digital Object Identifier 10.1109/JSTQE.2022.3223057

TABLE I
INFORMATION ON PATIENTS TREATED WITH ECMO IN THIS STUDY

	VV-ECMO (n = 22)	VA-ECMO (n = 22)
Age (years)	60.4 ±13.2	56.2 ± 15.2
Sex	M12/F10	M14/F8
BMI	26.4 ± 4.8	25.2 ± 5.1
Set time (days)	14 ± 9	11.9 ± 7.4
Mortality rate (%)	43.48	72.73

F, female; M, male; BMI, body mass index. BMI is the quotient of body weight in kilogram and the squared height in meter.

NIRS is a noninvasive optical method to evaluate regional oxygenation of the tissue circulation. Our preliminary study discussed patients' physiological status while undergoing ECMO and optimized ECMO therapy based on real-time peripheral NIRS probing [11]. This study continued the previous research methods to monitor hemoperfusion of patients' lower limb microcirculation. A feasibility study was conducted to evaluate the disease condition of patients receiving ECMO by combining NIRS data with a machine learning algorithm. In the future, we aim to develop an optical analysis system that assists in ECMO treatment, makes an objective assessment of prognosis and provides clinicians with more treatment information.

II. MATERIALS AND METHODS

The Institutional Review Board of Taipei Veterans General Hospital approved this study (TVGHIRB-2019-02-007AC). This approval is valid for two years, from Feb 12, 2019, until Feb 11, 2021. The study was conducted with adult patients (age >20 years) undergoing ECMO at Taipei Veterans General Hospital.

A. Patients

Patients undergoing VA-ECMO and VV-ECMO were included in this study. Patients in the following conditions were excluded from the study: (1) patients receiving ECMO with central cannulation; (2) patients for whom limbs were unsuitable for distal NIRS oximetry monitoring. Forty-four patients participated in this study, of which twenty-two patients were receiving VA-ECMO, and twenty-two patients were receiving VV-ECMO (Table I).

B. NIRS Measurement and Analysis

Hemodynamic responses were measured using two PortaLite systems (Artinis, Netherlands) at a distance from the ankle of approximately 60% of the tibia length (Fig. 1(a)). The instrument has three pairs of light sources and one photodetector. The distances between the sources and the detector are 30 mm, 35 mm, and 40 mm. The three light sources emit near-infrared rays at both wavelengths (760 nm and 850 nm). The light intensity data measured by the probe at a sampling rate of 25 Hz is transmitted to a computer via Bluetooth, and converted into the relative concentration changes of oxyhemoglobin (HbO_2, μ·M · minute^{-1}) and deoxyhemoglobin (HHb, μ·M · minute^{-1}), using PortaLite's dedicated software Oxysoft (Artinis, Netherlands). To determine absolute hemoglobin concentrations to estimate the tissue saturation index (TSI %), PortaLite employs spatially resolved spectroscopy (SRS). Subsequently, the blood oxygen information is filtered and normalized, and then brought into our machine learning algorithm.

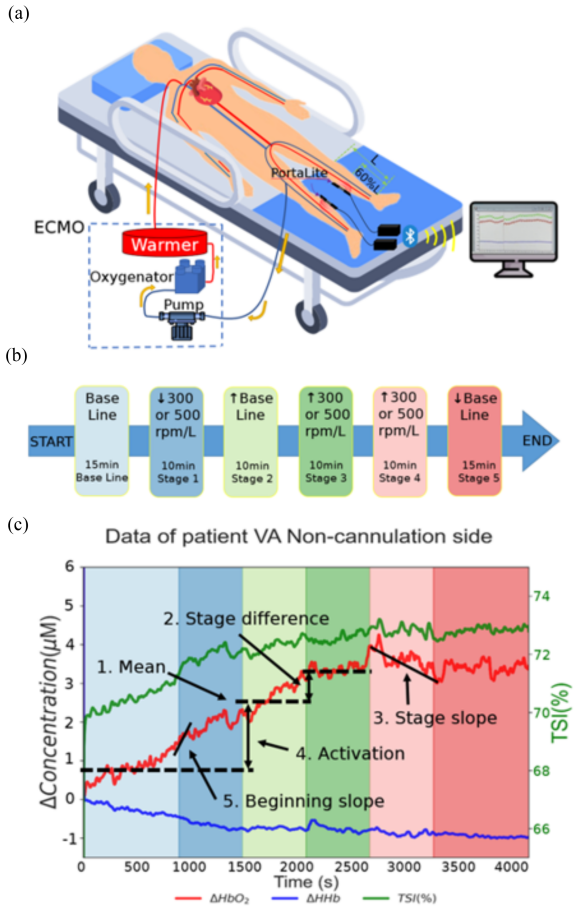

Fig. 1. (a) Measuring the lower limb approximately 60% of tibia length. (b) Experimental flowchart. (c) Schematic diagram of feature extraction of hemodynamics.

C. Measurement Protocol

At initiation, the ECMO flow rate was kept for 15 minutes (min) as the reference value to ensure the stability of the signal. In the VA-ECMO group, the flow rate was reduced by 500 revolutions per minute (rpm) for 10 min and returned to the initial flow rate for the next 10 min. Subsequently, the flow rate was increased by 500 rpm for 10 min and then by another 500 rpm for the next 10 min. Finally, the flow rate was returned to the original rate for 15 min (Fig. 1(b)). VA-ECMO needs to pump low-pressure venous blood to high-pressure arteries, so the adjusting pump speed unit in VA-ECMO is higher. In the VV-ECMO group, the adjustment protocol was the same as that for the VA-ECMO group, but each step made adjustments of 300 rpm. The adjustment criteria for determining the rotational speed of ECMO in the protocol are determined by the clinician's

experience. Makes changes in blood flow large enough to be observed without compromising patient safety. The PortaLite system monitored the patient for 70 min throughout the whole experiment.

D. Microcirculation Monitoring Results

Regardless of VA-ECMO or VV-ECMO, there is usually a cannula through the femoral vein or femoral artery on one side of the patient's leg in the ECMO device, so the lower limb of the patient could be divided into the cannulation side and the noncannulation side. The cannulation side greatly influences peripheral tissue hemoperfusion. Therefore, this study mainly discussed the changes in blood oxygen on the noncannulation side of the subjects.

E. Statistical Analysis

There are many periodic physiological signals in the raw data measured by NIRS, and these fixed-frequency physiological signals are the leading cause of the noise, including respiration (approximately 0.15–0.4 Hz) and heartbeat (approximately 0.4–1.6 Hz) [19]. We used an exponential moving average (EMA) to filter the signal to reduce the noise impact on the data analysis.

From the hemodynamic signal, the average values of HbO_2, HHb and TSI in each stage, stage slope, and stage beginning slope, and also calculate the activation degree and the stage difference for HbO_2 and HHb at each stage (Fig. 1(c)). These values were used as the classification model's characteristics, and the classification effectiveness was evaluated to select classification features with better discriminative ability.

1) Mean: Arithmetic mean of the blood perfusion values at each stage.
2) Stage difference: The difference between the average value of each stage and the average value of the previous stage.
3) Stage slope: The slope of the blood oxygen signal from the beginning to the end of each stage.
4) Activation degree: The difference between the average value of each stage and the average value of baseline.
5) Stage beginning slope: The slope of hemodynamic signal changes in the first 10 seconds after each stage. The reperfusion rate at the beginning of the stage was quantified as the slope change of the blood oxygen signal in the first 10 seconds based on the evaluation method of McClay et al. to evaluate the impact of instantaneous adjustment of ECMO speed at the beginning of the stage on micro-vascular reactivity [20].

After the above characteristic values were obtained, all data of individual features were scaled to the interval of [0, 1] according to the original proportion. This method can keep the original distribution characteristics of the original data and eliminate the significant differences caused by the individual differences between patients.

Support vector machine (SVM) is a set of supervised learning methods used for classification and regression. SVM is based on the structural risk minimization principle of statistical learning theory, which constructs a classification hyperplane in high-dimensional or infinite-dimensional space for classification and other tasks [21], [22], [23]. We use the radial basis function (RBF) as the model's nonlinear decision boundary's transformation function. The function can transform the input features into a high-dimensional feature space and solve some problems that linear functions cannot distinguish. The confusion matrix and k-fold cross-validation were used to test the model's classification performance and generalization ability.

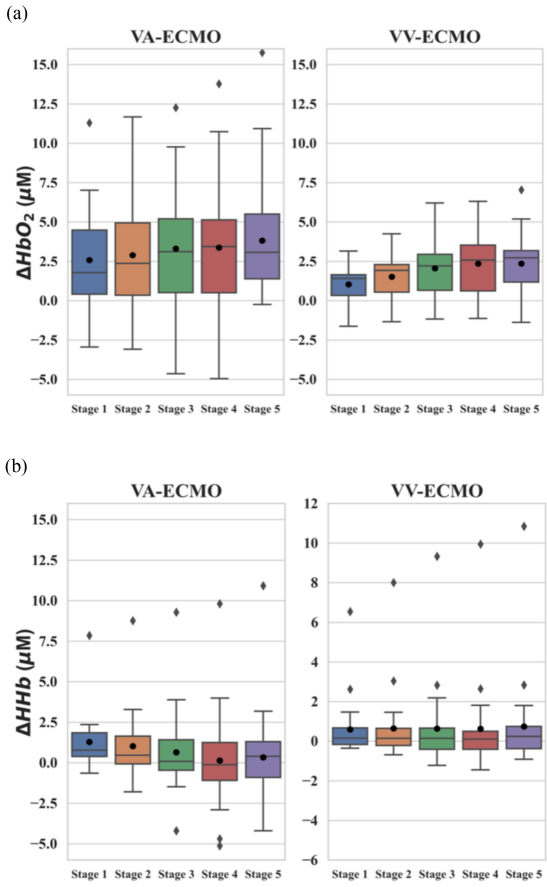

Fig. 2. Box plot of ΔHbO_2 (a) and ΔHHb (b) of patients receiving VA-ECMO and VV-ECMO. The black dot represents the mean changes in the concentration from baseline in each stage, and the diamond points outside represent outliers.

III. Results

A. Statistics Between VA and VV Groups

We classified as a discharge group for patients who successfully left the hospital after weaning from ECMO. Patients who could not wean from ECMO or passed away after weaning from ECMO were classified as the mortality group. In the VA group, their mean age was 56 years, and eight of them were female. In the VV group, ten were female, and their mean age was 60 years. The mortality rates were 72.73% (6 discharge/16 mortality) and 43.48% (12 discharge/10 mortality) in the VA and VV groups, respectively.

Fig. 2 shows the data distribution in every stage. The adjusting pump speed unit in VA-ECMO is higher than that in VV-ECMO in the experimental setting because VA-ECMO needs to pump low-pressure venous blood to high-pressure arteries, requiring a higher pump speed. Therefore, HbO_2 levels were higher in the

TABLE II
P VALUES OF CHARACTERISTICS IN THE VV-ECMO AND VA-ECMO GROUPS

VV-ECMO		VA-ECMO	
Feature	**P value**	**Feature**	**P value**
SBS_HbO_2_Stage5**	0.0090	SM_HbO_2_Stage2	0.0620
SD_HbO_2_Stage1*	0.0193	SM_HbO_2_Stage1	0.0788
SA_HbO_2_Stage1*	0.0230	SM_TSI_Stage5	0.1085
SD_HHb_Stage5*	0.0232	SM_TSI_Stage4	0.1112
SD_HbO_2_Stage4*	0.0293	SS_HHb_Stage5	0.1124
SD_HHb_Stage2*	0.0307	SS_HHb_Stage3	0.1189
SM_TSI_Stage3*	0.0353	SS_HHb_Stage1	0.1224

SBS, stage-beginning slope; SD, stage difference; SA, stage activation; SM, stage mean; SS, stage slope; *, $P \leq 0.05$; **, $P \leq 0.01$.

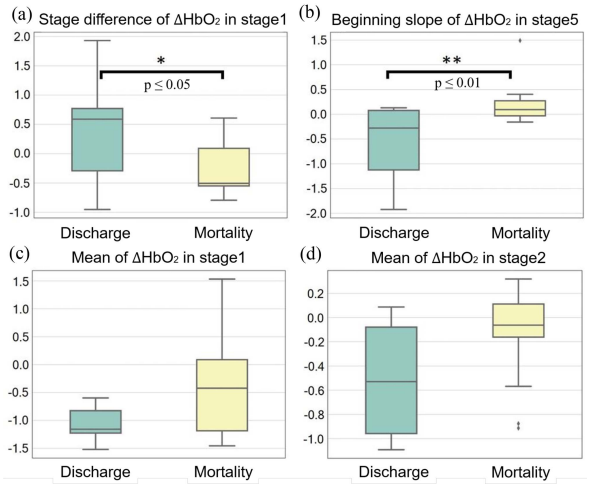

Fig. 3. Box plot of selected features in the VV-ECMO and VA-ECMO groups. Two chosen parameters from the VV-ECMO group were (a) Stage difference of ΔHbO_2 in stage 1 and (b) Beginning slope of ΔHbO_2 in stage 5. Two chosen parameters from the VA-ECMO group were (c) Mean of ΔHbO_2 in stage 1 and (d) Mean of ΔHbO_2 in stage 2.

VA-ECMO group than in the VV-ECMO group. From the box plot of the changes in HbO_2 and HHb concentrations of the two groups, the distribution of data in the VA group was relatively dispersed.

B. Feature Comparison and Extraction

After further analysis, we extracted 78 characteristic parameters from the NIRS signal on the noncannulation side of the VV-ECMO and VA-ECMO groups to classify the discharge and mortality groups. However, excessive input of useless feature parameters into the classification model will lead to overfitting the classification results. This research used an independent sample t test as a performance measure for machine learning algorithms. Table II lists the characteristic parameters selected from the VV-ECMO and VA-ECMO groups with better p values after comparison and ranking.

Fig. 3 illustrates the two sets of chosen parameters from the VV-ECMO and VA-ECMO groups and shows the distribution of these two sets of characteristic parameters in the discharge and mortality groups. We observed that the two features with better p values in the VV-ECMO group were the stage difference of ΔHbO_2 in stage 1 and the beginning slope of ΔHbO_2 in stage 5, both of which had statistically significant differences. In contrast, in the VA-ECMO group, the mean ΔHbO_2 in stage 1 and the mean ΔHbO_2 in stage 2 were extracted. However, the p values of the above characteristics were 0.0788 and 0.062, respectively, showing no statistically significant differences. Therefore, we could not prove that these two groups of characteristic parameters could be used as a reasonable basis for classification. Thus, we referred to Gottemukkula et al.'s research [24]. The team used receiver operating characteristic (ROC) curves and area under curve (AUC) values to rank NIRS signal features and selected the feature parameters with better performance to incorporate into the classification model. Table III shows the AUC values for the characteristics of the VV-ECMO and VA-ECMO groups.

TABLE III
AUC VALUES OF THE CHARACTERISTICS IN THE VV-ECMO AND VA-ECMO GROUPS

VV-ECMO		VA-ECMO	
Feature	**AUC**	**Feature**	**AUC**
SBS_HbO_2_Stage5	0.7778	SM_HbO_2_Stage2	0.7000
SD_HbO_2_Stage1	0.8148	SM_HbO_2_Stage1	0.7400
SA_HbO_2_Stage1	0.7593	SM_TSI_Stage5	0.7400
SD_HHb_Stage5	0.7593	SM_TSI_Stage4	0.7200
SD_HbO_2_Stage4	0.7593	SS_HHb_Stage5	0.6600
SD_HHb_Stage2	0.5556	SS_HHb_Stage3	0.5200
SM_TSI_Stage3	0.7407	SS_HHb_Stage1	0.5800

SBS, stage beginning slope; SD, stage difference; SA, stage activation; SM, stage mean; SS, stage slope; AUC = 0.5 (no discrimination); $0.7 \leq AUC \leq 0.8$ (acceptable discrimination); $0.8 \leq AUC \leq 0.9$ (excellent discrimination); $0.9 \leq AUC \leq 1.0$ (outstanding discrimination).

ROC is a probability curve, and AUC represents the degree or measure of separability. It tells how much the model is capable of distinguishing between classes. Therefore, the higher the AUC value, the more influential the evaluation features for the classification model [25], [26]. Table III showed that the two features, which were stage differences in ΔHbO_2 in stage 1 and stage beginning slope of ΔHbO_2 in stage 5, had better p values previously obtained in the VV-ECMO group. It still had a good performance in the ROC curve and the AUC value evaluation, with AUC values of 0.8148 and 0.7778, respectively (Fig. 4(a) and (b)), which had excellent discrimination. We extracted the stage mean of ΔHbO_2 in stage 1 and the stage difference for TSI % in stage 5 in the VA-ECMO group (Table III). Although both AUC features were 0.74, which indicated acceptable discrimination, the ROC curve's performance was abysmal (Fig. 4(c) and (d)).

C. SVM Classification Results

In this study, the VV-ECMO and VA-ECMO groups were included 22 subjects, respectively, and 70% of the data were used as a training set, and 30% as a testing set. After selecting the characteristic parameters with better discriminating ability, we built the SVM model to predict the outcome.

Fig. 5(a) and (b) shows the data distribution and model classification results of the VV-ECMO group classified by SVM under

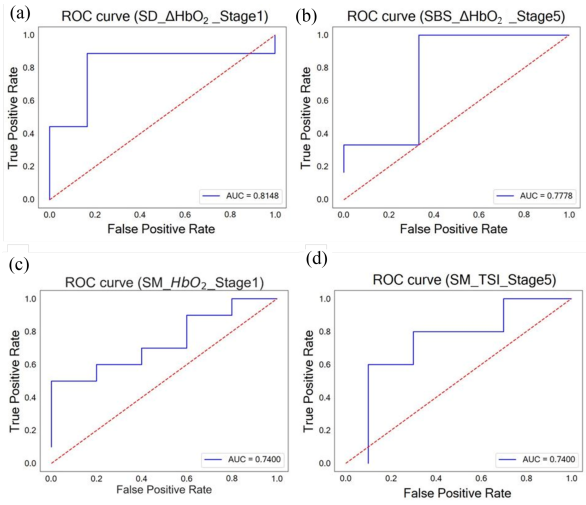

Fig. 4. The ROC curve and AUC value of the selected features in the VV-ECMO and VA-ECMO groups. The two features that had better AUC values in VV-ECMO and VA-ECMO were (a) Stage difference for ΔHbO_2 in stage 1 and (b) Beginning slope of ΔHbO_2 in stage 5. (c) Mean of ΔHbO_2 in stage 1 and (d) Mean of TSI % in stage 5.

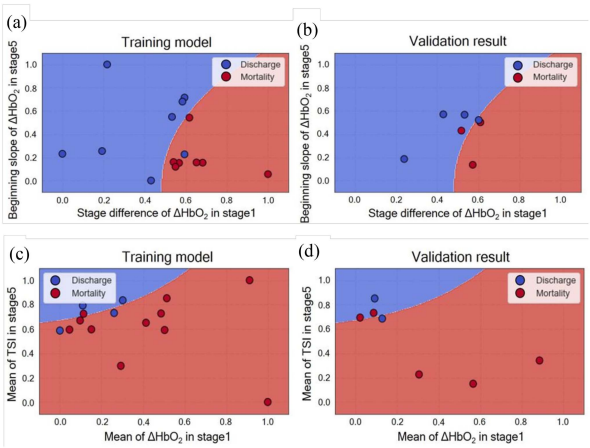

Fig. 5. The SVM results of the VV-ECMO and VA-ECMO groups. (a) VV-ECMO training model. (b) VV-ECMO testing set validation result. (c) VA-ECMO training model. (d) VA-ECMO testing set validation result.

two-dimensional features. The blue dots represent the discharge group's data, and the red dots represent the data points of the mortality group. The accuracy was 93.3% for the training set and 71.4% for the testing set.

Fig. 5(c) and (d) shows the data distribution and model classification results of the VA-ECMO group classified by SVM under two-dimensional features. In the same way as the VV-ECMO classification model mentioned above, the blue dots represent the discharge group's data points, and the red dots represent the data points of the mortality group. The accuracy was 86.7% for the training set and 57.1% for the testing set.

D. Result Validation

To prevent the deviation caused by the classification model's dependence on a specific training set or testing set, we need to test the classification performance and generalization ability of

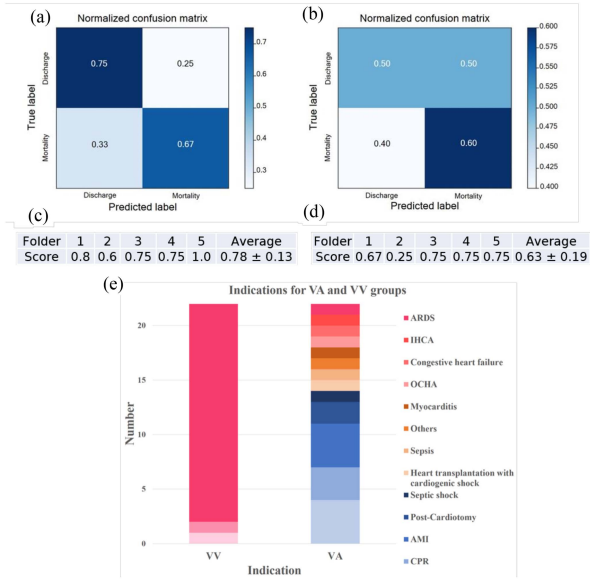

Fig. 6. The results of the VV-ECMO and VA-ECMO groups. Normalized confusion matrix of the (a) VV-ECMO classification model and (b) VA-ECMO classification model. The 5-fold cross-validation results of the VV-ECMO and VA-ECMO classification models were (c) 0.78 ± 0.13 and (d) 0.63 ± 0.19. (e) Indications for the VA and VV groups.

the two ECMO classification models using a confusion matrix and 5-fold cross-validation.

In the confusion matrix, the positive samples of the VV-ECMO testing set data label were three mortality patients, and the negative samples were four discharge patients. The matrix values were normalized to facilitate the observation of sensitivity and specificity results (Fig. 6(a)). The sensitivity and specificity of the proposed VV-ECMO classification model were 67% and 75%, respectively. The higher the two values are, the better the model's recognition for positive and negative samples. The five samplings' average accuracy and standard deviation in the 5-fold cross-validation were 0.78 ± 0.13 (Fig. 6(c)), indicating that the model had relatively good generalization ability and stability.

In the VA-ECMO classification model's confusion matrix, the positive samples of the testing set label were five mortality patients, and the negative samples were two discharge patients. The values of the matrix were also normalized. We observed that the VA-ECMO classification model's sensitivity and specificity were only 60% and 50%, respectively (Fig. 6(b)), while the average accuracy and standard deviation of 5-fold cross-validation were 0.63 ± 0.19 (Fig. 6(d)). The above model evaluation results indicate that the VA-ECMO classification model is relatively low in generalization ability and stability.

IV. Discussion

In the VV-ECMO classification model, we evaluated the feature's performance by the above method. We selected two features with better discriminative ability, namely, the stage difference of ΔHbO_2 in stage 1 and the beginning slope of ΔHbO_2 in stage 5. The two features showed a great difference between the two groups in VV-EMCO because the time point

in which these two features occur is when the microcirculation in the patient's body is more severely affected by the adjustment of the pump speed. When the patient has reached the final stage of physiological condition, the body's maintenance mechanism will concentrate blood to the body's core to ensure the functioning of vital organs such as the brain and liver. For the discharge group, the blood oxygen changes larger when affected by the pump speed adjustment; for the death group, the blood oxygen changes were small, and the measured characteristics of the two were significantly different. Thus, blood vessels such as peripheral arterioles, the peripheral circulatory system, and the intestinal system will constrict or close. Therefore, no matter how adjustments were made to the pump speed in ECMO, the hemoperfusion changes we measured were not significant. On the other hand, there are significant changes in blood oxygenation in the adjustment of the ECMO pump speed, which may indicate that the patient's peripheral regions can obtain sufficient oxygen for gas exchange between the cells and capillaries, help the damaged tissue to repair, and reduce the risk of complications. From the model's decision boundary (Fig. 5(a) and (b)), the two ethnic data points of VV-ECMO could be roughly separated, and there was no overfitting. Although it was not a very good classification result according to the accuracy of approximately 70% of the testing set classification, we believed that the classification error of the model at any data point would significantly affect the final result due to the insufficient amount of data collected at present. A small number of incorrectly classified data points appeared if we discussed the data distribution in the two-dimensional classification and the model's circle selection. Nevertheless, these data points are distributed near the model's decision boundary and have no extreme outliers. The normalized confusion matrix and 5-fold cross-validation show that the VV-ECMO classification model we built has relatively good classification generalization ability and model stability.

In the VA-ECMO classification model, the independent sample t test evaluation from the two groups in VA-ECMO failed to obtain statistically significant differences in characteristic values. Therefore, we referred to the relevant literature's feature selection methods and tried to use ROC curves and AUC values for feature evaluation. We selected two characteristic parameters with better AUC value performance, which were the stage mean of ΔHbO_2 in stage 1 and the stage mean of TSI % in stage 5. The model's decision boundary circled most of the discharge group's data points without overfitting (Fig. 5(c) and (d)). Nevertheless, several misclassified data points existed in the upper left corner of the training model. Even though the training set's classification model was approximately 90% accurate, we only obtained less than 60% accuracy when importing the testing data into the trained model. The results indicated that the classification model did not have good generalization ability in the VA-ECMO group classification. We believe that the reason for this result was that, on the one hand, the number of discharge populations of VA-ECMO collected in this study was insufficient. There was no statistically representative data distribution of the maternal population and no noticeable difference in distinguishing data, which led to the failure of proper fitting of the model. On the other hand, the poor performance of VA-ECMO classification results may be due to the complexity of the disease types of patients receiving this type of ECMO (Fig. 6(e)). For example, a patient suffering from shock due to severe bacterial infection and another patient suffering from myocarditis without bacterial infection received the same ECMO type. Patients' pathological changes and physiological responses were very different, so it was difficult to explain whether the blood oxygen changes measured in the same population were consistent. The normalized confusion matrix and 5-fold cross-validation results indicated that this model's classification performance and generalization ability did not meet the requirements. Therefore, it was impossible to distinguish the two groups of VA-ECMO from the present data.

This research work is a preliminary achievement of precision medicine of ECMO treatment. The ultimate goal of precision medicine is to minimize iatrogenic damage and minimize medical resource consumption to maximize the benefits of treatment. This research hopes to collect more data in the future, further refine the model and improve its performance, and predict whether the patient can be discharged from the hospital, which will provide a reference for clinicians. For patients who are predicted to be discharged from the hospital, better care should be given according to the actual situation; for patients who are predicted to death, it can also be considered whether to give up ineffective medical treatment.

V. Conclusion

This study is a preliminary feasibility study of the mechanism for evaluating patients' clinical conditions with ECMO. In VV-ECMO, we found that the construction of the classification model based on the characteristics of this type with better discriminating ability can effectively distinguish the two groups. The inspection of the classification model also shows that it has relatively good classification generalization ability and model stability. Regarding VA-ECMO, the complexity of the disease types and the insufficient amount of data did not lead to better results. Additionally, due to the classification accuracy, the classification model could only be used to make a preliminary assessment. More than 66.7% of patients are currently clinically equipped with VV-ECMO, indicating that the application of NIRS combined with machine learning has considerable potential. In the future, we hope to continue collecting more subjects to expand the ECMO patient database and improve the accuracy and generalization ability of the classification prediction model. After the model performance improves, more appropriate medical resources can be given to patients predicted to be discharged from the hospital, and unnecessary treatment can be reduced for patients predicted to death. We hope that this assessment tool will provide clinicians with a more accurate prediction of critically ill patients' conditions and effectively reduce the problems of medical resource abuse and ineffective care.

Appendix

Supplementary Video: https://drive.google.com/file/d/1tko5DTLfKQ7JGxHCtzSnkWrEf3clDPbF/view?usp = sharing

REFERENCES

[1] A. G. Tsai, P. C. Johnson, and M. Intaglietta, "Oxygen gradients in the microcirculation," *Physiol. Rev.*, vol. 83, pp. 933–963, Jul. 2003.

[2] C. Ince, "The microcirculation is the motor of sepsis," *Crit. Care*, vol. 9, pp. 1–7, Aug. 2005.

[3] A. S. Popel and P. C. Johnson, "Microcirculation and hemorheology," *Annu. Rev. Fluid Mech.*, vol. 37, pp. 43–69, Jan. 2005.

[4] B. R. Soller et al., "Oxygen saturation determined from deep muscle, not thenar tissue, is an early indicator of central hypovolemia in humans," *Crit. Care Med.*, vol. 36, pp. 176–182, Jan. 2008.

[5] D. Brodie and M. Bacchetta, "Extracorporeal membrane oxygenation for ARDS in adults," *New England J. Med.*, vol. 365, pp. 1905–1914, Nov. 2011.

[6] D. Fagnoul et al., "Extracorporeal cardiopulmonary resuscitation," *Curr. Opin. Crit. Care*, vol. 20, pp. 259–265, Jun. 2014.

[7] M. Y. Wu et al., "Using extracorporeal membrane oxygenation to rescue acute myocardial infarction with cardiopulmonary collapse: The impact of early coronary revascularization," *Resuscitation*, vol. 84, pp. 940–945, Jul. 2013.

[8] D. Abrams, A. Combes, and D. Brodie, "Extracorporeal membrane oxygenation in cardiopulmonary disease in adults," *J. Amer. College Cardiol.*, vol. 63, pp. 2769–2778, Jul. 2014.

[9] C. H. Wang et al., "Improved outcome of extracorporeal cardiopulmonary resuscitation for out-of-hospital cardiac arrest–a comparison with that for extracorporeal rescue for in-hospital cardiac arrest," *Resuscitation*, vol. 85, pp. 1219–1224, Sep. 2014.

[10] C. T. Huang et al., "Extracorporeal membrane oxygenation resuscitation in adult patients with refractory septic shock," *J. Thoracic Cardiovasc. Surg.*, vol. 146, pp. 1041–1046, Nov. 2013.

[11] H. H. Chang et al., "Optimization of extracorporeal membrane oxygenation therapy using near-infrared spectroscopy to assess changes in peripheral circulation: A pilot study," *J. Biophotonics*, vol. 13, Jul. 2020, Art. no. e202000116.

[12] G. Makdisi and I. W. Wang, "Extra corporeal membrane oxygenation (ECMO) review of a lifesaving technology," *J. Thoracic Dis.*, vol. 7, Jul. 2015, Art. no. E166.

[13] J. J. Squiers et al., "Contemporary extracorporeal membrane oxygenation therapy in adults: Fundamental principles and systematic review of the evidence," *J. Thoracic Cardiovasc. Surg.*, vol. 152, pp. 20–32, Jul. 2016.

[14] E. L. S. Organization. "ECLS registry report: International summary," 2020. Accessed: Jul. 21, 2020. [Online]. Available: https://www.elso.org/Registry/Statistics/InternationalSummary.aspx

[15] M. Schmidt et al., "Predicting survival after ECMO for refractory cardiogenic shock: The survival after veno-arterial-ECMO (SAVE)-score," *Eur. Heart J.*, vol. 36, pp. 2246–2256, Sep. 2015.

[16] R. Cheng et al., "Complications of extracorporeal membrane oxygenation for treatment of cardiogenic shock and cardiac arrest: A meta-analysis of 1,866 adultpatients," *Ann. Thoracic Surg.*, vol. 97, pp. 610–616, Feb. 2014.

[17] Y. Y. Juo et al., "Efficacy of distal perfusion cannulae in preventing limb ischemia during extracorporeal membrane oxygenation: A systematic review and meta-analysis," *Artif. Organs*, vol. 41, pp. E263–E273, Aug. 2017.

[18] C. Bauer et al., "Extracorporeal membrane oxygenation with danaparoid sodium after massive pulmonary embolism," *Anesth. Analg.*, vol. 106, pp. 1101–1103, Apr. 2008.

[19] Z. Li et al., "Spectral analysis of near-infrared spectroscopy signals measured from prefrontal lobe in subjects at risk for stroke," *Med. Phys.*, vol. 39, pp. 2179–2185, Mar. 2012.

[20] K. M. McLay et al., "Repeatability of vascular responsiveness measures derived from near-infrared spectroscopy," *Physiol. Rep.*, vol. 4, May 2016, Art. no. e12772.

[21] G. Cauwenberghs and T. Poggio, "Incremental and decremental support vector machine learning," *Adv. Neural Inf. Process. Syst.*, vol. 13, pp. 409–415, 2001.

[22] S. Tong and D. Koller, "Support vector machine active learning with applications to text classification," *J. Mach. Learn. Res.*, vol. 2, pp. 45–66, Nov. 2001.

[23] P. Panja et al., "Least square support vector machine: An emerging tool for data analysis," in *Proc. SPE Low Perm Symp., Soc. Petroleum Eng.*, 2016, pp. 4–11, Paper SPE-180202-MS.

[24] V. Gottemukkula and R. Derakhshani, "Classification-guided feature selection for NIRS-based BCI," in *Proc. 5th Int. IEEE/EMBS Conf. Neural Eng.*, 2011, pp. 72–75.

[25] J. Huang and C. X. Ling, "Using AUC and accuracy in evaluating learning algorithms," *IEEE Trans. Knowl. Data Eng.*, vol. 17, no. 3, pp. 299–310, Mar. 2005.

[26] J. A. Swets, *Signal Detection Theory and ROC Analysis in Psychology and Diagnostics: Collected Papers*. London, UK: Psychology Press, 2014.

Hsiao-Huang Chang was born in 1965. He received the B.S. degree in medicine from Taipei Medical University, Taipei, Taiwan, in 1991, and the Ph.D. degree from Berlin University, Berlin, Germany, in 2006. From 1991 to 1998, he went to Taipei Veterans General Hospital and finished full cardiovascular surgery and intensive care training. In 1998, he became an Attending Cardiovascular Surgeon. He went to the German Heart Center, Berlin, for advanced training, for two years. His main research interests include calcification, Raman spectroscopy, intensive care, heart transplantation, and artificial hearts.

Yung-Chang Chen was born in 1999. He received the B.Sc. degree in electrical engineering from Feng Chia University, Taichung, Taiwan, in 2021. He is currently working toward the M.Sc. degree with the Biomedical Optical Imaging Laboratory, Department of Photonics, National Yang Ming Chiao Tung University, Hsinchu, Taiwan. His research focuses on developing near-infrared spectroscopy device to study the clinical diseases.

Ting-Wei Chiang was born in 1997. She received the B.Sc. degree from the Department of Physics, National Sun Yat-sen University, Kaohsiung, Taiwan, in 2019, and the M.Sc. degree from the Department of Photonics, National Yang Ming Chiao Tung University, Hsinchu, Taiwan, in 2021.

Yi-Min Wang received the M.Sc. Degree from the Department of Physics, National Sun Yat-sen University, Kaohsiung, Taiwan, in 2001, and the Ph.D. degree from the Institute of Photonics and Optoelectronics, National Taiwan University, Taipei, Taiwan, in 2009. He is currently a Postdoctoral Researcher with the Department of Photonics, National Yang Ming Chiao Tung University, Hsinchu, Taiwan. His research interests include intelligent biophotonic techniques, diffuse optical tomography, near-infrared spectroscopy, optical coherence tomography, and clinical applications based on biomedical optical imaging techniques.

Chia-Wei Sun was born in Taiwan, China, in 1975. He received the B.Sc. degree in electrical engineering from National Cheng Kung University, Tainan, Taiwan, in 1997, the M.Sc. degree in biomedical engineering from National Yang-Ming University, Taipei, Taiwan, in 1999, and the Ph.D. degree from the Institute of Photonics and Optoelectronics, National Taiwan University, Taipei, Taiwan, in 2003. He is currently the Director with the Institute of Biomedical Engineering and a Professor with the Department of Photonics, National Yang Ming Chiao Tung University, Hsinchu, Taiwan. He has contributed to more than 80 peer-reviewed journal papers. His research interests include intelligent biophotonics, functional optical imaging, functional optical coherence tomography, neurophotonics, and clinical applications based on biomedical optical imaging techniques.